

Numerical comparison of bearing capacity of tapered pile groups using 3D FEM

Nader Hataf* and Amin Shafaghat^a

Department of Civil and Environmental Engineering, Shiraz University, Shiraz, Iran

(Received October 17, 2014, Revised May 12, 2015, Accepted May 18, 2015)

Abstract. This study investigates the behavior of group of tapered and cylindrical piles. The bearing capacities of groups of tapered and cylindrical piles are computed and compared. Modeling of group of piles in this study is conducted in sand using three-dimensional finite element software. For this purpose, total bearing capacity of each group is firstly calculated using the load-displacement curve under specific load and common techniques. Then, the model of group of piles is reloaded under this calculated capacity to find group settlements, stress states on the lateral surfaces of group block, efficiency of group and etc. In order to calculate the efficiency of each group, single tapered and cylindrical piles are modeled separately. Comparison for both tapered and cylindrical group of piles with same volume is conducted and a relation to predict tapered pile group efficiency is developed. A parametric study is also performed by changing parameters such as tapered angle, angle of internal friction of sand, dilatancy angle of soil and coefficient of lateral earth pressure to find their influences on single pile and pile group behavior.

Keywords: group of pile; tapered pile; bearing capacity; 3D modeling; finite element

1. Introduction

Pile groups with vertical loading

When several piles are grouped together, it is expected that the soil pressures produced from either side friction or point bearing of each pile overlap. Intensity of additional pressure depends on pile load and their distances and if they sufficiently grow, the soil will fail in shear or some additional settlements will occur. As pile distances increase, stress intensity in overlapped stress areas clearly decreases. Usually the cap of pile group is constructed to support structure columns and also to distribute load on piles evenly. Therefore, the long pile distances are often impractical.

Considering few numerical studies, modeling tapered piles and pile group, in comparison with more experimental studies, this study aims to model the tapered and cylindrical pile group by three-dimensional software "PLAXIS". Having modeled the pile group, some properties of piles, including tapering angle, friction angle of sand soil, coefficient of lateral earth pressure, and dilatancy angle of soil are changed and results are then compared. It should be noted that for tapered pile, tapering angle is increased from 0 to 1.6°. During the modeling stages, the length of

*Corresponding author, Professor, E-mail: nhataf@shirazu.ac.ir

^a Graduate Student, E-mail: shafaghat@shirazu.ac.ir

all piles and their spaces in pile groups, optimally selected, kept constant. Modeling is performed for a 4-pile group. Having obtained load-settlement curves, total bearing capacity of each group is measured using various and common techniques and again pile group is analyzed under that force. Then, the results of secondary analysis are obtained and a numerical integration on the surface of pile tip is performed. This is conducted by transferring series of data related to effective vertical stress to “surfer 2009”, commercial software, in order to determine the values of end bearing capacity and pile friction.

2. Literature review

2.1 Laboratory and in-situ tests

To investigate the axial behavior of tapered piles a laboratory study was conducted by Wei and El Naggar (1998). They highlighted the economic advantage of tapered piles under static loading conditions. They expected the body resistance to increase by increasing tapering angle and that occurred. They reported body resistance of tapered piles is 40% more than that for cylindrical piles. The differences between both kinds of piles decreased for higher amount of confining pressure and load distribution in length of pile body for both piles was identical. They realized that the length to pile upper diameter ratio of tapered piles should not exceed more than 20. Wide experimental research program has been done for studying the effectiveness of tapered piles by El Naggar and Wei (1999a). They have recognized that tapered piles have a more efficient distribution of materials than piles with constant section. For tapered piles with depth of more than 20 times of pile diameter, the negative effect in “uplift” bearing capacity severely decreases. Hence the role of tapered piles is not ignorable and they have the potential to be compared with cylindrical piles in this regard. According to the results of experimental tests and investigations on statically loaded tapered piles, the following points were established:

- A. Bearing capacity of both types of cylindrical and tapered piles increases as lateral pressure increases.
- B. In high lateral pressures, the tapering effect decreases.
- C. Shear stresses between soil and pile through all lateral surfaces of pile increase due to increase of radius in tapered piles which contributes to application of more pressure on adjacent sand.
- D. End bearing strength of tapered piles is less than that for a pile with straight wall.

Furthermore the behavior of tapered piles was investigated by conducting centrifuge tests (El Naggar and Sakr 2000). To provide optimal efficiency for tapered piles, the results of these tests have suggested that the relation of pile cone length to upper diameter of pile should not exceed 20 to 25. Robinsky and Morrison also performed some experimental tests (Robinsky and Morrison 1964). Norlund has realized that through lateral friction, a tapered pile can bear bigger loads than a pile with straight wall in relatively uniform and non-cohesive soils (Nordlund 1963). Tests on in-situ large scale tapered piles also conducted and the results are offered by Norlund, D’Appolonia and Hribar, and Rybnikov (Nordlund 1963, D’Appolonia and Hribar 1963, Rybnikov 1990). The axial behavior of tapered piles and also their bearing capacities are studied by Paik *et al.* (Paik *et al.* 2011). The results of their tests indicated that the frictional load of tapered pile continuously increases by increasing pile settlement. Although in cylindrical piles, in a settlement

of about 2% of pile diameter, this value reaches to its final value. Piles' tapering angle and properties of soil can change the proportion of bearing capacity of tapered piles to cylindrical piles. Without considering soil conditions, final body resistance of tapered pile is more than cylindrical ones, whereas the final end load of tapered piles in dense sand is more than cylindrical ones, when lateral coefficient of earth pressure is more than 0.42. It is also perceived that regardless of relative density and stress condition in sand, with the increase of tapering angle, end bearing due to pile length increases. According to experimental models' results, tapered factors are offered and suggested for frictional bearing due to its length and final bearing which are used for estimation of bearing capacity of tapered piles. A series of experimental tests have also been done on single tapered piles by Ghasemi (2006). Another case study to investigate the bearing capacity of piles is performed by Eslami and Fellenius (1997).

2.2 Numerical and analytical investigations

Although several experimental tests are conducted for studying the behavior of these piles, there are a few numerical modeling on tapered piles. A numerical study is performed for assessing the bearing capacity of tapered piles and step-tapered piles under axial loading (Ghazavi and Lavasan 2006). In 2012, in this area, another numerical survey on single tapered piles is performed (Zhan *et al.* 2012). Two series of single tapered piles under axial loading in sand are analyzed using FEM in order to investigate their behavior. It is observed that as taper angle increases, resistance of body increases, but the advantage of tapered piles comparing to cylindrical ones was observed only in sand with low dilatancy. For tapered piles there is an optimum tapered angle in homogenous sand which their bearing capacity is 12% more than their cylindrical counterpart piles. Bearing capacity directly increases as tapered angle increases when weaker sediment exists beneath the tip of pile. Another conclusion is that as floating foundations, tapered piles have a better application. Analytical solutions are suggested by Bakholdin, Kodikara and Moore for determination of bearing capacity of tapered piles (Bakholdin 1971, Kodikara and Moore 1993). Moreover, other technical and computational researches have been performed on the bearing capacity of piles using FEM and other methods (Khan *et al.* 2008, El Naggar and Wei 1999b, 2000, Veiskarami *et al.* 2011, Fattah *et al.* 2015, Ren *et al.* 2014).

3. Methodology of the research

3.1 The properties of used piles and soils

In this study, since the aim is comparing the bearing capacity of the same volume cylindrical and tapered piles, the focus is on the method that considers the volume of a cylindrical reference pile constant and changes its upper and lower cross sections. In such a way, the pile tip cross section gradually becomes smaller and the upper cross section enlarges. So piles with the same volume and different tapering angles are made and their geometry properties are represented in Table 1. The cylindrical reference pile of 10 meters long and 60 centimetres diameter is considered.

Properties of the soil are given in Table 2.

In sand, the focus is more on the soil internal friction angle, dilatancy angle and lateral pressure coefficient.

Table 1 The properties of modeling tapered piles

PILE	α (degree)	R_B (m)	R_T (m)	L (m)	V (m ³)
C1	0	0.3	0.3	10	2.8
T1	0.4	0.26	0.33	10	2.8
T2	0.8	0.23	0.37	10	2.8
T3	1.2	0.19	0.4	10	2.8
T4	1.6	0.15	0.43	10	2.8

Table 2 The properties of used sand in modeling

Parameter	Sand
Dry unit weight, $\gamma_d \left(\frac{kN}{m^3} \right)$	17
Saturated unit weight, $\gamma_{sat} \left(\frac{kN}{m^3} \right)$	20
Material model	Hardening soil
Elastic modulus, E (MPa)	30
Friction angle, ϕ'	33°
Cohesion, C' (kPa)	0
Dilatancy angle, ψ	3°
Lateral pressure coefficient, K_o	0.45
Poisson's ration, ν	0.2
Interface coefficient, R_{INTER}	0.7

Table 3 Different considered cases for modeling in sand

Case	1 st	2 nd	3 rd	4 th	5 th
ϕ (°)	33	38	43	33	33
ψ (°)	3	8	13	3	3
K	0.45	0.45	0.45	0.7	0.95

Therefore for conducting sensitivity analysis, the friction angle (ϕ), dilatancy angle (ψ), and lateral pressure coefficient (K_o), are changed as indicated in Table 3.

3.2 Finite element modelling

In this study the software PLAXIS 3D is used which is a general geotechnical finite element program with a full 3D preprocessor that allows cad objects to be imported and further processed within a geotechnical context was used for analysis. The modes enable a realistic simulation of construction and excavation processes by activating and deactivating soil volume clusters and structural objects, application of loads, changing of water tables, etc.

3.3 Dimensions of borehole

In numerical modeling for considering borehole dimensions where piles represent a behavior like when they are in the ground, some conditions should be provided. Therefore, dimensions are considered at least in a way that the stress distribution beneath and around piles can be as real. For prevention of direct effect of boundaries on analysis, suitable dimensions should be implemented for model or cluster. Soil cluster dimensions should be included in height as $2.5 L$ and in width as $(1-\nu) 2.5 L$ (Vesic 1967), where L is the embedment length of the pile and ν is the Poisson's ratio of soil. In this study, for more exact calculation cluster dimensions of $3 L$ in height and width are considered. Fig. 1 illustrates stress range around block of pile group.

3.4 Cluster meshing

For model meshing, 10-node triangular elements were used which have high accuracy in analysis of subjects. For soil cluster, average or medium mesh sizes were used. Using refine option, the elements were changed into very tiny ones to increase accuracy of piles' model and their interface planes, soil, and also soil within group block between piles' model which bears high amount of stress. Sensitivity analysis to meshing was performed for a pile model for clarification of effect of meshing in calculation accuracy. Fig. 2 indicates three dimensional view of the block of pile group.

3.5 Pile group models

Modeling of pile group was conducted using the geometry shown in Fig. 3.

Pile distance in group is of great importance in calculation, results and behavior of group. In this study, optimal distance was used, which is $3D$, where D is average diameter of considered tapered piles (Vesic 1975).

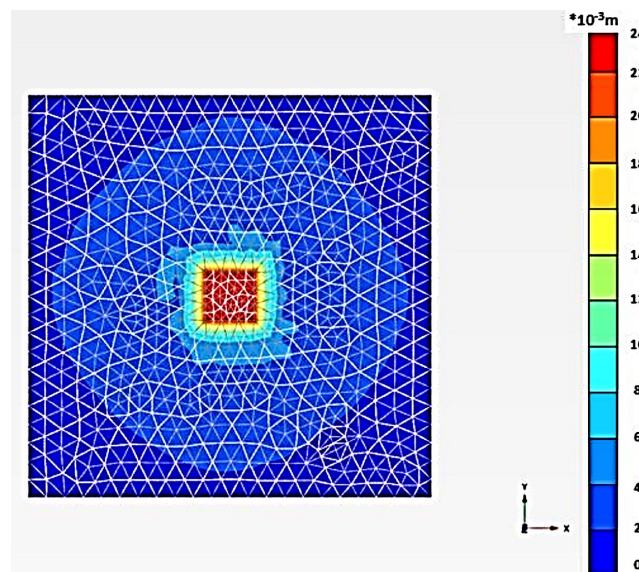


Fig. 1 Cluster plan and pile group vertical displacement within it

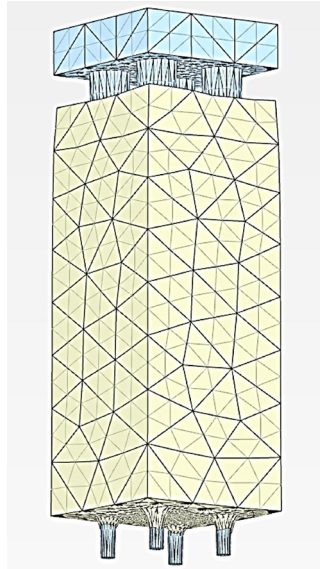


Fig. 2 Block of meshed pile group with different size

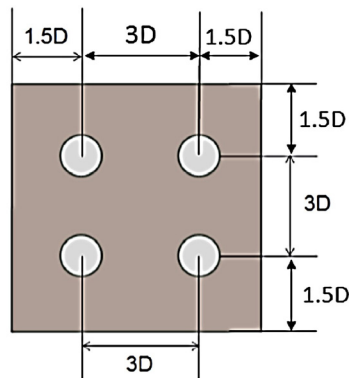


Fig. 3 Plan of pile group and their arrangement in group

For creating the cap of pile group, $1.5D$ (where D is mean diameter of piles) for the distance of cap verge of pile group to center of each pile in each corner is used.

In modeling of pile group, 5 group series are analyzed and each series includes 5 pile groups. In each series of modeling, 5 model groups including a quadric cylindrical group, named GC1 and four tapered pile group with angles of 0.4° , 0.8° , 1.2° , and 1.6° , named GT1 to GT4 with same volume are analyzed. Within each series, all variables except the one which is under consideration, kept constant. Pile groups are analyzed under the same condition. In the first series $\phi = 33^\circ$, $\psi = 3^\circ$, and $K_s = 0.45$. For other series these parameters were changed. Therefore, three series of pile group with different ϕ , ψ and also three series with different lateral pressure coefficients are analyzed and then compared. It should be noted that comparisons are made either for models within a series and/or with models of other series.

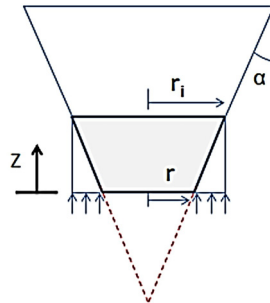


Fig. 4 End bearing force along the body of each tapered pile

3.6 The analysis method

To obtain the bearing capacity of each pile group, two analyses using PLAXIS 3D software are conducted. Firstly, each pile group was loaded to about two times of estimated capacity obtained through manual calculation relations. After the first analysis is finished, the load-settlement diagram is obtained as output of the program. Then the bearing capacity of each single pile and pile group is calculated using various methods, Tangent Intersection method and Davisson method (Us army corps of engineers 1997, Whitaker 1957). Then the single pile or the pile group is analyzed under the load capacity value which has obtained from their own load-displacement curves to observe stress distribution proportional to specific bearing capacity of each model at the end of pile or around the pile body or even block of pile group.

Fifty analyses for pile group and thirty for single piles were performed by considering this procedure during the study. The analysis of single piles is done just by changing the internal friction angles and dilatancy angle of soil and the analyses of single pile models considering changing in the soil lateral pressure coefficient are neglected. After loading the models of single pile or pile group to their load capacity, the surface of piles' tip can be considered as a plane in outputs of program. Then the distribution of effective normal stress is achieved in elements of that plane related to about 313 elements or nodes.

Now using surfer 2009 and entering the data and numerical integration on this plane, the amount of pressure on this plane and in addition many other properties of pile tip plane can be observed, including 3D map of stress distribution on this plane or even topography of its effective stress. It should be noticed that this program provides different methods for numerical integration and Kriging was found the most suitable method for this study (Surfer 8 user's manual version 4.1 2009). After calculation of end bearing capacity of pile, the side friction capacity of pile can be obtained.

It is also notable that due to inclined body of tapered piles, these piles can provide end bearing capacity along their length, Fig. 4.

According to Fig. 4, the value of end bearing due to inclined body of tapered piles can be calculated by integration on its surface along its length.

4. Results and discussions

As mentioned before this work sheds light on investigation and numerical comparison of

bearing capacity of same volume tapered and cylindrical pile groups in sand under different conditions of pile, soil and geometry. It also presents a relationship for efficiency of tapered and cylindrical pile groups and their comparison with other relations and also comparing of settlement factor for each pile group to relationships presented by Vesic (Hanna *et al.* 2004).

4.1 Pile groups in sand with different internal frictions

In the first series of models, there are five pile groups including one cylindrical group and four tapered groups are compared. Additionally, cylindrical pile group in first series can be compared to cylindrical ones of second and third or fourth and fifth. It should be mentioned that for considering the effect of piles' cap on load capacity, a loose and soft layer beneath cap is used.

The load-settlement curves obtained numerically for tapered and cylindrical pile groups (i.e., Four piles in a group) in sand with different internal friction angles are shown in Figs. 5 and 6 and 7. These figures are related to sands with internal friction angle of 33° , 38° and 43° , respectively. It should be mentioned that the GC in these figures stands for cylindrical pile groups and GT stands for tapered pile groups. Vertical axis indicates vertical compressive force (kN) acting over

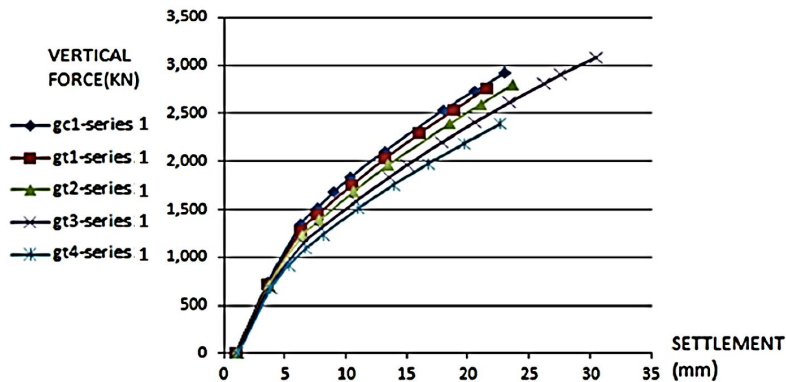


Fig. 5 The load-settlement curves for tapered and cylindrical pile groups in sand with internal friction angle of 33 degrees

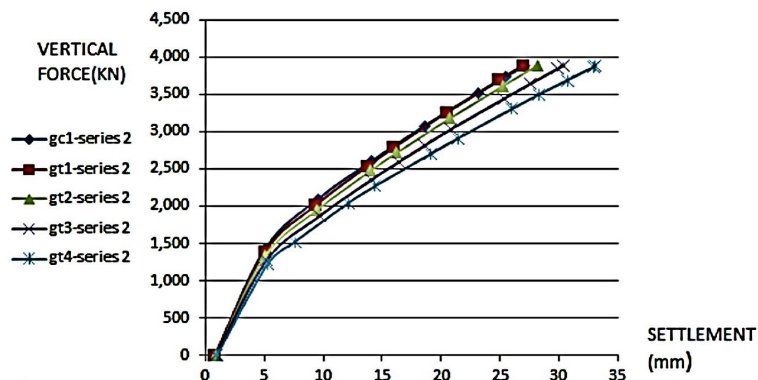


Fig. 6 The load-settlement curves for tapered and cylindrical pile groups in sand with internal friction angle of 38 degrees

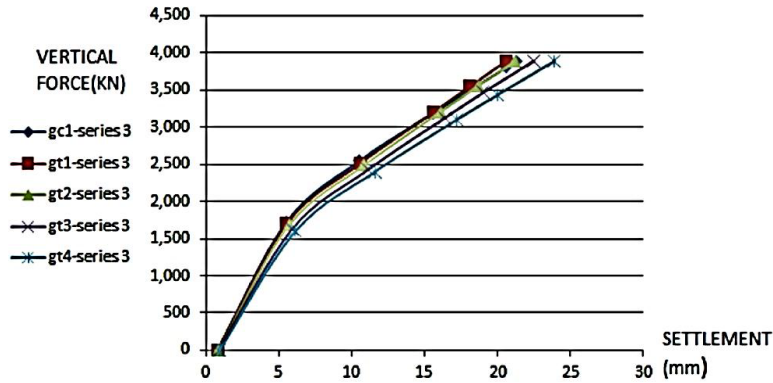


Fig. 7 The load-settlement curves for tapered and cylindrical pile groups in sand with internal friction angle of 43 degrees

cap of pile groups and horizontal axis indicates the settlement of pile groups in millimeters.

As it can be seen in diagrams of Figs. 5 and 6 and 7, in the first set of diagrams which is plotted for sand with internal friction angle of $\phi = 33^\circ$, the pile groups shows elastic behavior up to the load of 1200 kN and this value for pile groups placed in sand with $\phi = 38^\circ$ and $\phi = 43^\circ$ are 1500 kN and 2000 kN, respectively. Therefore, the load capacity increases severely as internal friction angle in sand increases. For investigating the block behavior of tapered and cylindrical pile groups, the output of PLAXIS in terms of the stresses related to end plane of each pile in group as points' coordinates is obtained and then it is transferred to Surfer 2009. In this software, the end surface of each pile can be plotted three-dimensionally and the condition of effective normal stress on that plane is shown by different methods. In this research, a three dimensional stress distribution view of piles' tip represented and it indicates the stress distribution in different points of pile tip. The following figures show these planes for three piles, a cylindrical and two tapered with tapering angles of $\alpha = 0.8^\circ$ and 1.6° in sand with internal friction angle of $\phi' = 33^\circ$.

As it can be seen in diagrams of Figs. 5 and 6 and 7, in the first set of diagrams which is plotted for sand with internal friction angle of $\phi = 33^\circ$, the pile groups shows elastic behavior up to the load of 1200 kN and this value for pile groups placed in sand with $\phi = 38^\circ$ and $\phi = 43^\circ$ are 1500 kN and 2000 kN, respectively. Therefore, the load capacity increases severely as internal friction angle in sand increases. For investigating the block behavior of tapered and cylindrical pile groups, the output of PLAXIS in terms of the stresses related to end plane of each pile in group as points' coordinates is obtained and then it is transferred to Surfer 2009. In this software, the end surface of each pile can be plotted three-dimensionally and the condition of effective normal stress on that

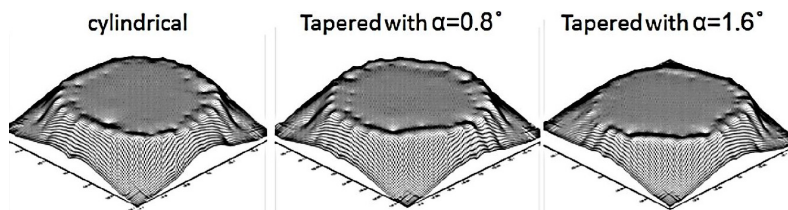


Fig. 8 3D distribution of stress over end surface of tapered and cylindrical piles

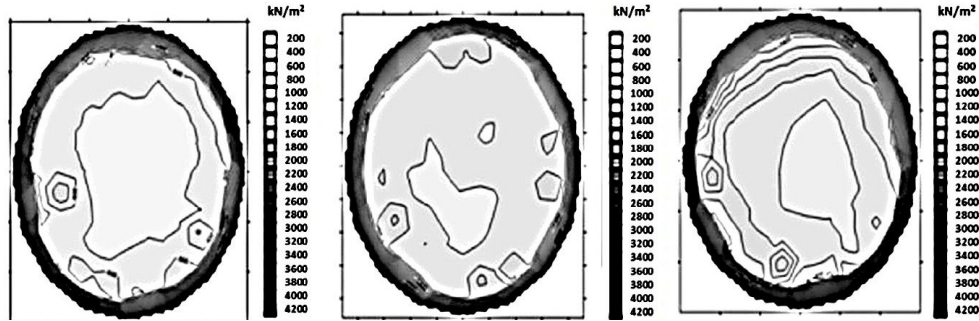


Fig. 9 Stress contours on end surface of tapered and cylindrical piles of the same volume

plane is shown by different methods. In this research, a three dimensional stress distribution view of piles' tip represented and it indicates the stress distribution in different points of pile tip. The following figures show these planes for three piles, a cylindrical and two tapered with tapering angles of $\alpha = 0.8^\circ$ and 1.6° in sand with internal friction angle of $\phi' = 33^\circ$.

As the above diagrams show, for cylindrical pile lower stress value in the center of its end plane, states an inefficient stress distribution on the end surface of pile. While for pile with tapering angle of $\alpha = 0.8^\circ$, the stress distribution is more efficient. Because the stress is distributed on all parts of the plane and the center of it can bear loads. This status presents an effective total bearing of tapered piles. For third condition, that is tapered pile with tapering angle of $\alpha = 1.6^\circ$, the stress distribution is not monotonous and stress contours are very close to each other and they are combined with many changes. This shows that bearing capacity of this pile type is not efficient and it doesn't provide more bearing capability.

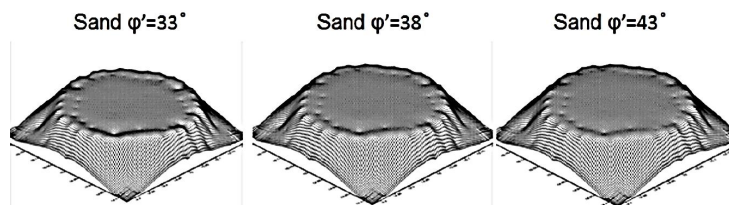


Fig. 10 3D stress distribution on final surface of tapered and cylindrical piles

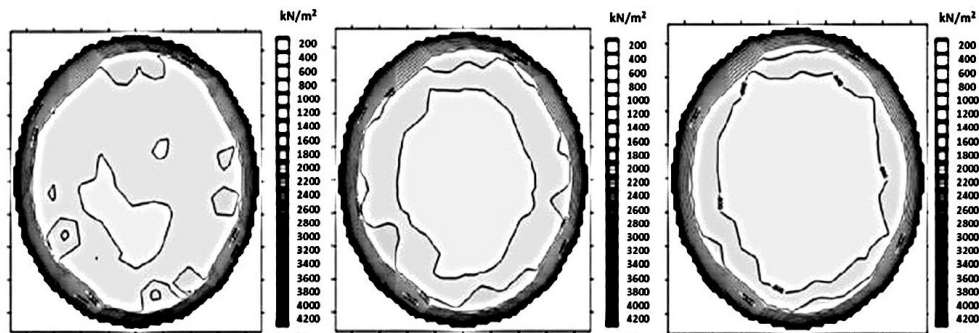


Fig. 11 Stress contours on end surface of tapered piles in sand with different internal friction angle

In another case, the situation of effective stress in end plane of a tapered pile in three conditions of sand with internal friction angles of $\phi' = 43^\circ$, $\phi' = 38^\circ$, and $\phi' = 33^\circ$ are placed next to each other in order to make a comparison for effective stress distribution in this plane for a pile in various conditions of sand.

As it can be seen in the figures, as internal friction angle of sand increases, stress distribution is not decreased in verges of pile end plane and the bearing resistance is increased by increasing the soil friction angle. In this case, by presenting the condition of effective stress in pile end plane in the form of stress contour, the case will become clearer. In Fig. 11 the conditions of stress contour are shown for a tapered pile with tapering angle of $\alpha = 0.8^\circ$, and in three conditions with $\phi' = 43^\circ$, $\phi' = 38^\circ$, and $\phi' = 33^\circ$.

As the above figures indicate, by increasing the soil internal friction angle, there is an area in the central of pile end surface which is spreading. This area which is shown with a lighter color indicates that stress distribution grows monotonously in pile end plane and bearing of tapered pile increases as the soil internal friction angle increases. Whereas bearing increases by growing of the soil internal friction angle, frictional bearing of tapered piles increases intensely in medium and dense sand. This alone can be a verification of tapered pile effectiveness. Table 4 indicates the values of end bearing for a tapered pile (with tapering angle of 0.8°) placed in sand with different internal friction angles. This Table consists of three columns. In the first column that entitles the "Frictional Bearing", the values are showing the frictional bearing of a tapered pile with tapering angle of 0.8° in sand with three different internal friction angles of 33° , 38° , 43° . The second column that entitles "End Bearing" is showing the sum of end bearing capacities of tapered pile due to its end surface and inclined body. In fact tapered piles can have an end bearing capacity along their body and this value will increase as the tapering angle increases. As in this study, the main purpose is to compare the bearing capacity of group of tapered piles, the end bearing capacity of tapered piles along their length was calculated using analytical solutions and finally it was added to the end bearing of piles which was calculated by SURFER software.

Since tapered piles have inclined body, by increasing the load on their head, the soil surrounding their body will be compact. This compactness will lead to a more soil lateral pressure around the inclined body and will increase the normal force on the inclined body surface of these piles. Hence, despite the fact that tapered piles (comparing to their same volume cylindrical piles) have less lateral surface area for providing frictional bearing capacity, it can be seen that they have higher frictional bearing capacity.

Due to this fact, for soils with different internal friction angles the trend of bearing capacity will be different. Since the rate of this trend of changing in bearing capacity decreases as the soil internal friction angle decreases, it can be predicted that for tapered piles in sand with lower internal friction angles as $\phi = 28^\circ$, $\phi = 23^\circ$ changing in the trend of bearing capacity be much lower and tapered piles would not suggest for using instead of their same volume cylindrical ones in such soils.

Table 4 The values of end and frictional bearing capacity of tapered pile with tapering angle of 0.8°

Frictional bearing	End bearing	The sand internal friction angle
164 kN	183 kN	33°
228 kN	206 kN	38°
295 kN	219 kN	43°

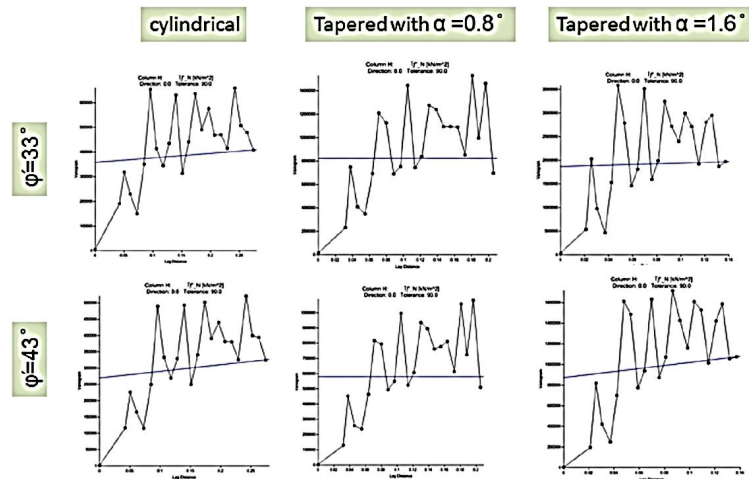


Fig. 12 Variograms of effective stress in end surface of tapered and cylindrical pile in two kinds of sand

4.2 Comparison of variograms

One of the applications of Surfer software is to draw the variograms related to variable inputted the program in terms of distance. For clarification and making a relation with existing variables of this study, that is data of effective normal stress, the related variograms of these parameters are plotted in end plane of piles as follows.

Above variograms are related to three piles in the form of tapered and cylindrical with tapering angle of $\alpha = 0.8^\circ$ and $\alpha = 1.6^\circ$ in two kinds of sand with $\phi = 43^\circ$ and $\phi = 33^\circ$. As it can be seen, stress distribution in sand with $\phi = 33^\circ$ for tapered piles is in a more steady state from center of pile end plane. In fact, variograms are variance diagrams of effective stress difference in two different points of pile end surface in terms of distance. In sand with $\phi = 43^\circ$, the best state of effective stress distribution is occurred according to steadiness for tapered pile with tapering angle of $\alpha = 0.8^\circ$.

4.3 The comparison of bearing capacity of pile group in sand

By modeling and analyzing of pile group in sand with different conditions of internal friction angle, it can be found that the bearing capacity of pile groups strongly depends on internal friction angle. As predicted, by increasing the soil internal friction angle, the elastic behavior of pile group acts in a wider range and it shows higher bearing values. For more clarification, the force-settlement diagrams of each pile presented in previous parts are about 1250, 1500, and 2000 kN, for internal friction angles of $\phi = 33^\circ$, 38° , and 43° , respectively. It can be seen that for pile groups as internal friction angle of sand increases, the elastic behavior range increased.

The comparisons are conducted for five four-pile groups which include a cylindrical group and four tapered groups with different coefficient and lateral pressures of $K_0 = 0.45$, $K_0 = 0.7$, and $K_0 = 0.95$. For this comparison, the pile groups are located in sand with constant internal friction angle of $\phi = 33^\circ$. The elastic behavior of pile groups reaches to 1250, 1750, and 2750 kN, respectively. Figs. 13 and 14 and 15 indicate the force-settlement diagrams for cylindrical and tapered pile

groups together for various states of lateral pressure coefficient of $K_0 = 0.45, K_0 = 0.7,$ and $K_0 = 0.95$ in sand respectively.

From above figures, it can be realized that the implementation of tapered and even cylindrical pile by driven method is accompanied with increasing of more bearing capacity than cast-in-place method.

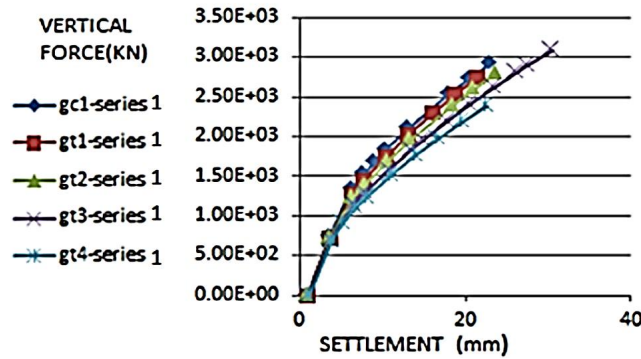


Fig. 13 The force-settlement diagrams of pile groups in sand with $k_0 = 0.45$

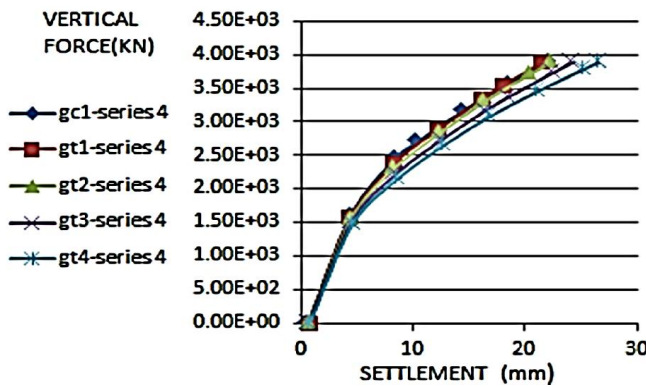


Fig. 14 The force-settlement diagrams of pile groups in sand with $k_0 = 0.7$

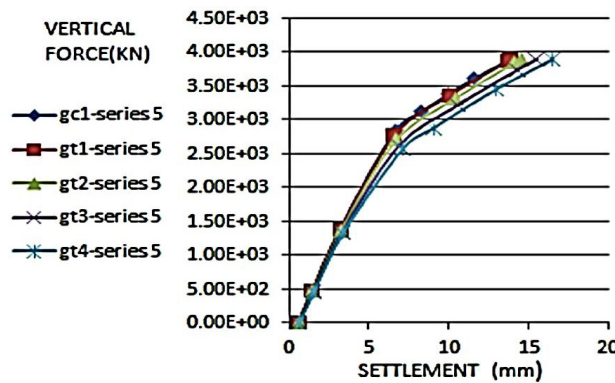


Fig. 15 The force-settlement diagrams of pile groups in sand with $k_0 = 0.95$

4.4 Efficiency of pile group

In this study, the bearing capacity of pile group is obtained by the Tangent intersection method and Davisson's method. Then, single corresponding piles and pile group are separately modeled and analyzed under their specific bearing capacity. Then, using the below equation, the efficiency of each pile group is calculated

$$\eta = \frac{Q_{ug}}{n.Q_{us}} \quad (1)$$

Where Q_{ug} is total obtained bearing capacity for pile group, Q_{us} is total obtained bearing capacity for single pile, n is the number of existing pile in group and η is the group efficiency. For each pile group and all three sand types with $\phi' = 43^\circ$, $\phi' = 38^\circ$, and $\phi' = 33^\circ$, these values are calculated and they are plotted in a diagram in which vertical axis is efficiency of pile group and the horizontal one is tapering angle of tapered pile. By fitting a line for each series of pile group in three sand types, an efficiency equation is obtained for cylindrical and tapered pile group in terms of tapering angle in sands with different internal friction angle. Moreover, a general efficiency equation of four-pile group in sand will be achieved by averaging of these three efficiency equations and also it is accompanied with supposing the optimal distance proportional to $3D$ where D is the mean diameter of piles. Fig. 16 clearly indicates this matter.

After the calculation of bearing capacity of pile groups and also single piles of each group, the efficiency of each group is calculated using Eq. (1) and they are plotted in a diagram in terms of tapering angle. Then by practicing a diagram on obtained points, efficiency equations can be achieved for each series of pile group in sand with different internal friction angles as follows

$$\text{Sand with internal friction angle of 33 degrees: } \eta_1 = -0.187\alpha + 1.357 \quad (2)$$

$$\text{Sand with internal friction angle of 38 degrees: } \eta_2 = -0.152\alpha + 1.368 \quad (3)$$

$$\text{Sand with internal friction angle of 43 degrees: } \eta_3 = -0.091\alpha + 1.319 \quad (4)$$

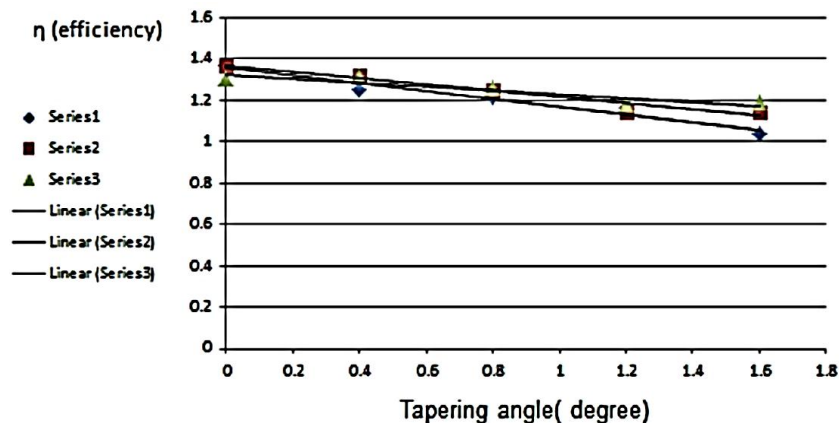


Fig. 16 Efficiency diagram of presented cylindrical and tapered pile group of this study in terms of tapering angle

By a simple approximation, above equations can be rewritten as one efficiency equation in terms of soil friction and tapering angle as follows

$$\eta_3 = (0.34 \cdot \tan\phi - 0.41) \cdot \alpha + 1.35 \tag{5}$$

Simplifying Eqs. (2) to (4) is contributed to an efficiency Eq. (5) for cylindrical and tapered pile groups considering the assumption of four piles with optimal spacing of 3D in groups, where D is the average diameter of piles, α is the tapering angle, and ϕ is the soil internal friction angle. Furthermore, another approximation is considered and the Eq. (5) can be written roughly as

$$\eta = -0.143\alpha + 1.348 \tag{6}$$

4.5 Comparison of developed relation for efficiency of pile group with other offered relationships

As it was noted in previous sections, so far many equations are offered for determining the efficiency of cylindrical pile groups. Every equation considers special conditions of pile position in group, pile cap, etc. For example, the well-known Converse-Labbare equation considers that the pile cap is not placed on the ground surface. Vesic equations are defined for 4-pile and 9-pile in group, but in either cases, the group cap is placed on ground surface. In 1965, Kishida and Meyerhof didn't consider the proportion of L/D in efficiency of pile groups where L and D are the length and depth of pile respectively (Hanna *et al.* 2004, Vesic 1969, Kishida and Meyerhof 1965).

For making a comparison of proposed relation in this study and other presented equations, the efficiency of pile group was calculated from each equation with similar conditions. In this study, pile group includes four piles and pile cap was considered to be located on ground surface. The pile distances were the same for all cases. The group efficiency related to different methods can be seen in Table 5.

As the results indicate, for efficiency of cylindrical 4-piles group in which cap is located on the soil surface, group efficiency is equal to 1.66, 0.89 for Vesic, Converse-Labbare relations, respectively. In the case that the pile group cap with four piles is placed over the soil surface, the

Table 5 Comparison of pile group efficiency with different methods

Method	Vesic With CAP	Converse-Labbare Free-Standing CAP	Kishida-Meyerhof With CAP	Brand et.al with CAP	Presented method With CAP on soft soil
Efficiency	1.66	0.89	$0.8 \leq \eta \leq 1.6$	$1 \leq \eta \leq 1.2$	1.35

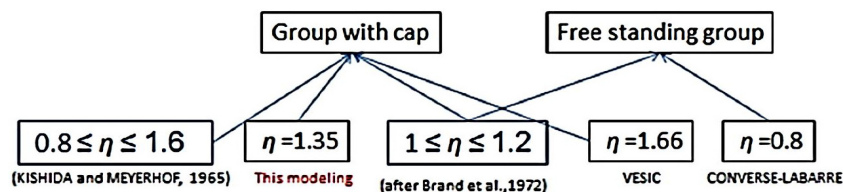


Fig. 17 Categorization of efficiency equations in terms of considering pile group cap

efficiency of pile group is about 1.35 using the present study relation which is reasonable. While offered relations of this study can calculate the efficiency of tapered pile group by considering their tapering angle, other relations are offered only for cylindrical piles. In general, offered equations for efficiency of pile group can be categorized as Fig. 17.

4.6 Frictional and end bearing efficiency of piles

For calculating frictional and bearing efficiency of tapered and cylindrical pile group, the values of end bearing due to inclined tapered body should be considered. In fact during the calculation of frictional bearing, the value of end bearing, which is achieved using numerical integration on the piles tip surface, is subtracted from total bearing and the remain value is the sum of frictional and end bearing of body due to the inclination along pile length. So the value of the end bearing along the body is a part of achieved value for frictional bearing which should be subtracted. After calculating the body efficiency and pile end bearing, the below diagrams are plotted which are the efficiency in terms of pile tapering angle. The following diagrams are plotted for sand with three different states of tapering angle. Figs. 18 and 19 and 20 indicate the friction

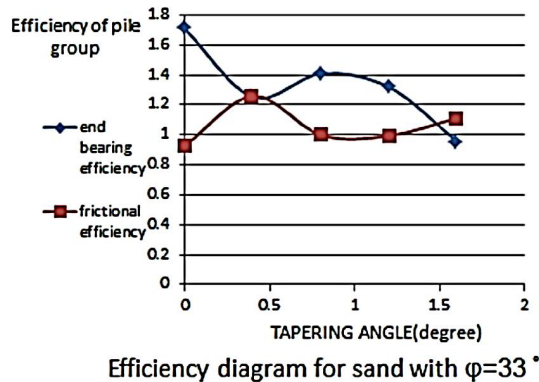


Fig. 18 Diagram of friction and end bearing efficiency of pile group in sand with internal friction angle of 33°

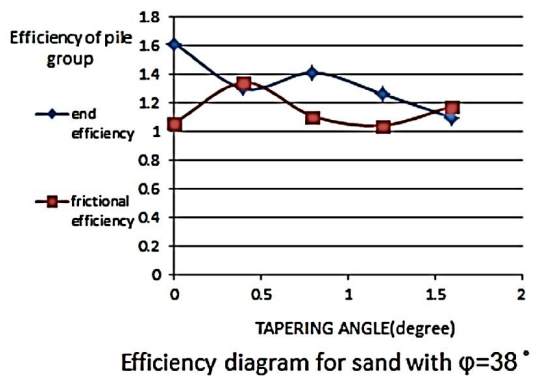


Fig. 19 Diagram of friction and end bearing efficiency of pile group in sand with internal friction angle of 38°

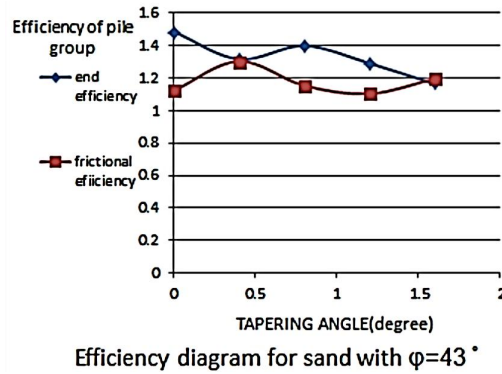


Fig. 20 Diagram of friction and end bearing efficiency of pile group in sand with internal friction angle of 43°

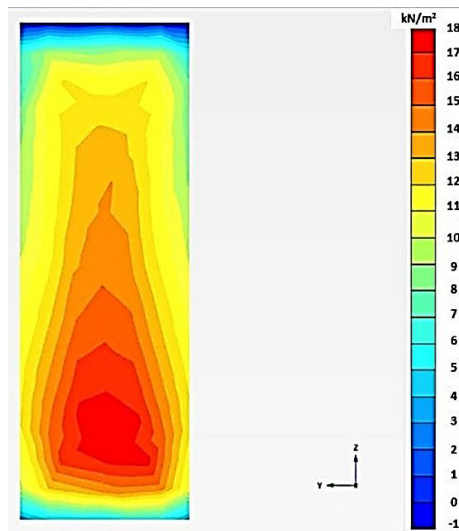


Fig. 21 Shear stress distribution on the lateral wall of block of cylindrical pile group

and end bearing efficiency of pile group in sand with internal friction angle of 33° , 38° and 43° .

According to above diagrams, as internal friction angle of sand increases, the values of body efficiency and end of pile get close each other. This means that by increasing the soil internal friction angle, tapered piles act more optimal in frictional and end bearing and therefore they can provide more bearing capacity.

4.7 The shear stress on block wall planes of pile group

In order to observe the stress condition in pile group modeling, the interface plane between soil lateral wall of block of pile group and its surrounding soil were considered. The stress condition on these planes for both cylindrical and tapered piles with same volume and tapering angle of 1.6° in sand is shown in the following figure. Figs. 21 and 22 indicate shear stress distribution on lateral wall of block of cylindrical and tapered pile group, respectively.

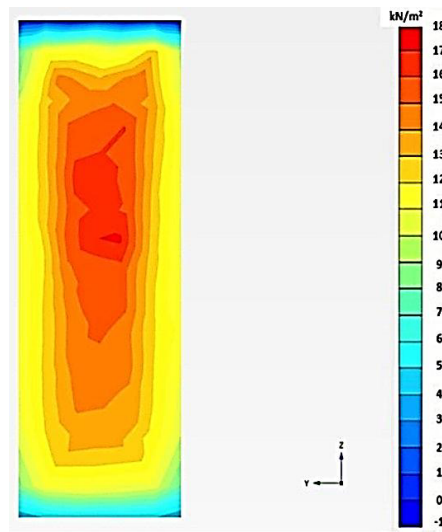


Fig. 22 Shear stress distribution on the lateral wall of block of cylindrical pile group

As it can be seen in above figures, for cylindrical piles, the value of shear stress is higher in lower parts of planes, whereas for tapered piles the stress value is higher in upper parts of planes. The reason may be due to the greater thickness of tapered piles in upper parts compared to that for cylindrical piles.

4.8 Stress in block end planes of pile group without considering the end surface of the piles

In order to observe the effective stress condition perpendicular to defined common interface planes of end of block in pile group and soil, interface planes with soil should be defined during

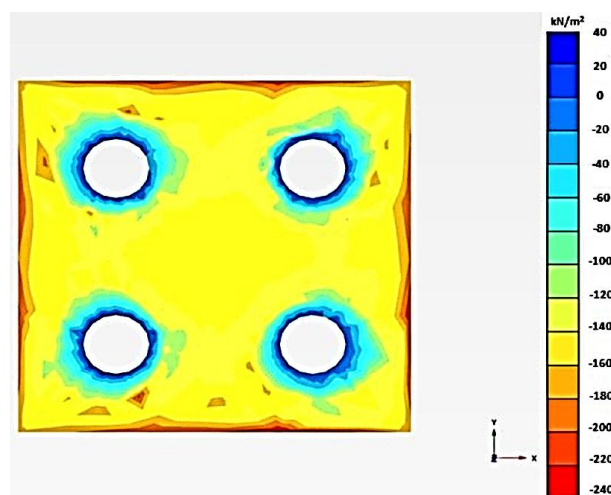


Fig. 23 Vertical stress distribution on block end surface of cylindrical pile group

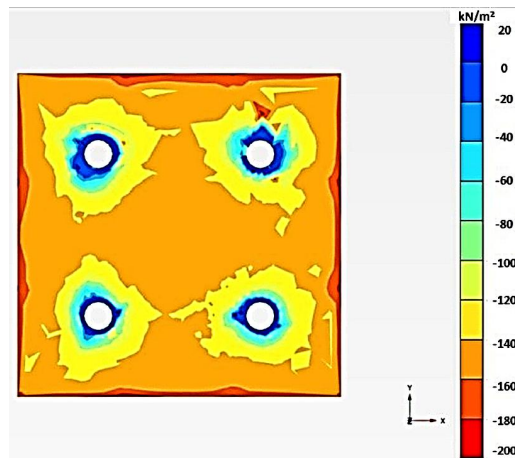


Fig. 24 Vertical stress distribution on block end surface of tapered pile group

modeling for end part of block in pile group without considering pile end surface. In following figures, these planes can be observed. These are plotted for cylindrical and tapered pile group with tapering angle of 1.6° in sand and internal friction angle of 43° . Figs. 23 and 24 illustrates the effective vertical stress distribution on block end surface of cylindrical and tapered pile group without considering pile end surface.

According to above figures, it can be found that for cylindrical piles that have more end bearing due to bigger end surface, end plane of block of pile group experiences less stress, but for tapered piles, this plane relatively experiences more effective vertical stress

5. Conclusions

According to data related to bearing capacity and settlement of cylindrical and tapered pile group and also single piles used in each group in sand, the following results can be achieved.

- (1) As the soil internal friction angle increases, tapered groups with higher tapering angle will have higher bearing capacity. So for sands of $\phi = 38^\circ$ and $\phi = 43^\circ$, bearing capacity of tapered piles with tapering angle 0.4° and 0.8° are more than other same volume piles. In this case, for sand with $\phi = 33^\circ$, bearing capacity of cylindrical pile group is more than tapered piles.
- (2) For pile group with $\phi = 38^\circ$ and $\phi = 43^\circ$, the increase in bearing capacity of tapered piles comparing to same volume cylindrical pile is about 0.7% and 5% that respectively occurred for tapered piles of 0.4° and 0.8° .
- (3) For tapered pile group, increasing of soil lateral pressure coefficient contributes to increase of bearing capacity very much that this matter is an evident of more optimal use of tapered pile as driven piles. The increasing of bearing capacity with lateral pressure coefficient of 0.7 and 0.95 comparing $K_0 = 0.45$ in sand with $\phi = 33^\circ$ is about 42% and 75%.
- (4) Using tapered piles in soils with bigger internal friction angle is more optimal and it is not recommended in cohesive soils.

- (5) As tapering angle increases, efficiency of tapered pile group decreases. The rate of efficiency of tapered pile group decreases as the sand internal friction angle increases.

Acknowledgments

Authors would like to thank Professor Arsalan Ghahramani for his golden experiences which were keys of solving many problems of this study. Thanks to Fateme Nematollahi for her invaluable support and help.

References

- Bakholdin, B.V. (1971), "Bearing capacity of pyramidal piles", *Proceedings of the 4th Conference on Soil Mechanics and Foundation Engineering*, Budapest, Hungary, pp. 507-510.
- D'Appolonia, E. and Hribar, J.A. (1963), "Load transfer in step-tapered piles", *Soil Mech. Found. Div., ASCE*, **89**(6), 57-77.
- El Naggar, M.H. and Wei, J.Q. (1999a), "Axial capacity of tapered piles established from model tests", *Can. Geotech. J.*, **36**(6), 1185-1194.
- El Naggar, M.H. and Wei, J.Q. (1999b), "Response of tapered piles subjected to lateral loading", *Can. Geotech. J.*, **36**(1), 52-71.
- El Naggar, M.H. and Sakr, M. (2000), "Evaluation of axial performance of tapered piles from centrifuge tests", *Can. Geotech. J.*, **37**(6), 1295-1308.
- El Naggar, M.H. and Wei, J.Q. (2000), "Uplift behavior of tapered piles established from model tests", *Can. Geotech. J.*, **37**(1), 56-74.
- Fattah, M.Y., Yousif, M.A. and Al-Tameemi, S.M.K. (2015), "Effect of pile group geometry on bearing capacity of piled raft foundations", *Struct. Eng. Mech., Int. J.*, **54**(5), 829-853.
- Eslami, A. and Fellenius, B.H. (1997), "Pile capacity by direct CPT and CPTu methods applied to 102 case histories", *Can. Geotech. J.*, **34**(6), 886-904.
- Ghasemi, M. (2006), "Experimental investigation of bearing capacity of pyramidal piles in sand", M.Sc. Thesis; Soil Mechanics & Foundation, Yazd University, Iran.
- Ghazavi, M. and Lavasan, A.A. (2006), "Bearing capacity of tapered and step-tapered piles subjected to axial compressive loading", *Proceedings of the 7th International Conference on Coasts, Ports & Marine Structures*, ICOPMAS, Tehran, Iran.
- Hanna, A.M., Morcous, G. and Helmy, M. (2004), "Efficiency of pile groups installed in cohesionless soil using artificial neural networks", *Can. Geotech. J.*, **41**(6), 1241-1249.
- Khan, M., Kamran, M., El Naggar, H. and Elkasabgy, M. (2008), "Compression testing and analysis of drilled concrete tapered piles in cohesive-frictional soil", *Can. Geotech. J.*, **45**(3), 377-392.
- Kishida, H. and Meyerhof, G.G. (1965), "Bearing capacity of pile group under eccentric loads in sand", *Soil Mech. Fdn. Eng. Conf. Proc.*, Canada.
- Kodikara, J.K. and Moore, I.D. (1993), "Axial response of tapered piles in cohesive frictional ground", *Geotech. Eng.*, **119**(4), 675-693.
- Nordlund, R.L. (1963), "Bearing capacity of piles in cohesionless soils", *Soil Mech. Found. Div., ASCE*, **89**(3), 1-36.
- Paik, K., Lee, J. and Kim, D. (2011), "Axial response and bearing capacity of tapered piles in sandy soil", *Geotech. Test. J.*, **34**(2), 122-130.
- Ren, Q.X., Hou, C., Lam, D. and Han, L.H. (2014), "Experiments on the bearing capacity of tapered concrete filled double skin steel tubular (CFDST) stub columns", *Steel Compos. Struct., Int. J.*, **17**(5), 667-686.
- Robinsky, E.L. and Morrison, C.F. (1964), "Sand displacement and compaction around model friction piles",

- NRC Research; *Can. Geotech. J.*, **1**(2), 81-93. DOI: 10.1139/t64-002
- Rybnikov, A.M. (1990), "Experimental investigations of bearing capacity of bored-cast-in-place tapered piles", *Soil Mech. Found. Eng.*, **27**(2), 48-52.
- Surfer 8 user's manual version 4.1 (2009), Copyright Golden Software, USA.
- Us army corps of engineers (1997), EL 02 CO97, US Army Publication, USA.
- Veiskarami, M., Eslami, A. and Kumar, J. (2011), "End-bearing capacity of driven piles in sand using the stress characteristics method: Analysis and implementation", *Can. Geotech. J.*, **48**(10), 1570-1586.
- Vesic, A.S. (1967), "Ultimate loads and settlements of deep foundations in sand", Duke University, Durham, NC, USA.
- Vesic, A.S. (1969), "Experiments with instrumented pile groups in sand", Duke University, School of Engineering.
- Vesic, A. (1975), "Bearing capacity of shallow foundations", *Foundation Engineering Handbook 3*, pp. 121-145.
- Wei, J. and El Naggar, M.H. (1998), "Experimental study of axial behavior of tapered piles", *Can. Geotech. J.*, **35**(4), 641-654.
- Whitaker, T. (1957), "Experiments with model piles in groups", *Geotechnique*, **7**(4), 147-167.
- Zhan, Y.G., Wang, H. and Liu, F.C. (2012), "Numerical study on load capacity behavior of tapered pile foundations", *Electron. J. Geotech. Eng.*, **17**, 1969-1980.